

A flat and cost effective actuator based on superabsorbent polymer driving a skin attachable drug delivery system

Michael Vosseler¹, Markus Clemenz¹ and Roland Zengerle^{1,2,3}

¹ HSG-IMIT, Wilhelm-Schickard-Straße 10, D-78052 Villingen-Schwenningen, Germany

² Laboratory for MEMS Applications, Department of Microsystems Engineering—IMTEK, University of Freiburg, Georges-Koehler-Allee 106, D-79110 Freiburg, Germany

³ BIOS Centre for Biological Signalling Studies, University of Freiburg, D-79110 Freiburg, Germany

E-mail: michael.vosseler@hsg-imit.de


Received 9 March 2012, in final form 6 July 2012

Published 27 July 2012

Online at stacks.iop.org/SMS/21/105002

Abstract

We present a flat and cost effective volume displacement actuator based on superabsorbent polymer. It offers slow kinetics and is able to work against reasonable back-pressures, e.g. 0.50 ml in 235 min at 140 kPa. It is predestined for low-cost skin attachable drug delivery devices. The actuator consists of a plastic ring filled with superabsorbent polymer granulate. It is sealed with a thermoplastic elastomeric membrane on one side and a stiff filter membrane on the other side. After adding a defined amount (e.g. 2 or 10 ml) of swelling agent the actuator shows a fast initial volume displacement within a few minutes followed by a slow continuous increase of this volume within hours. Minimized initial volume displacement and maximized displaced volume after 4 h cannot be combined in one actuator. A minimized initial displacement can be as low as 0.10 ml ± 0.03 ml. A maximized displaced volume after 4 h can be 1.71 ml ± 0.18 ml, not considering the initial effect. The back-pressure dependency of one selected actuator design was studied. At a back-pressure of 100 kPa the displaced volume is reduced by 33%. We investigated various actuator designs with varying surface area, hardness of the elastomeric membrane and superabsorbent polymer. Finally, we demonstrate a skin attachable drug delivery system based on the employment of the superabsorbent polymer actuator.

 Online supplementary data available from stacks.iop.org/SMS/21/105002/mmedia

(Some figures may appear in colour only in the online journal)

1. Introduction

Drug delivery devices facilitate transport of drug molecules into the body. The term device is used for a broad range of different technologies. Many devices contain the drug in its solid form. Pills and transdermal therapeutic systems are the most prominent examples [1, 2]. Other devices contain a drug solution that is injected or infused into the body. Syringes and infusion pumps are the most prominent examples in this category. Infusion pumps are usually connected to intravenous or subcutaneous infusion sets. However, hollow

microneedles for intradermal infusions are currently under investigation [3–5].

Currently, there is a trend to miniaturize infusion pumps. Such pumps are supposed to be light in weight and flat. The light weight is necessary so that it can stick to the skin without the risk of falling off. The flat design is important for discrete wearability and comfort. If these two criteria are fulfilled, an infusion pump is called a ‘patch pump’. For diabetic patients, such pumps need to be programmable with bolus functions. However, there are applications where such comprehensive functionality is not necessary. A slow infusion process is

required e.g. for highly viscous antibody solutions that cannot be injected.

There are quite a lot of different actuation technologies for infusion pumps. Actuators can be as simple as a spring⁴ [6] or an elastic membrane⁵. Pumps with gas generators are also state-of-the-art⁶. Electromechanical syringe drivers are used when there are demanding requirements on the flow rate and/or occlusion detection is necessary. A short review of the literature shows that these technologies are usually not considered as suitable mechanisms for patch pumps in various company and university laboratories.

Micropumps, typically actuated with piezoactuators, are frequently used for small drug delivery devices [7–9]. However, the expensive micro-fabrication technologies used to manufacture such pumps usually inhibit the development of disposable devices. Thus, technologies with reduced needs of expensive micro-technologies are investigated. A compound material based on expancells [10] is able to transform thermal energy into mechanical work and results in a volume expansion. Another smart solution is based on a battery expanding its volume and is developed by Steadymed⁷.

The Medipad infusor is based on a pressurized gas generated by a controlled electrolysis process [11, 12]. Its approximate dimensions are 8.5 cm × 6.2 cm × 2.1 cm with a mass of less than 50 g. The flat design of the device is persuasive. Volunteers considered it comfortable to wear. Drug solution can be infused e.g. at 42 $\mu\text{l h}^{-1}$ for 24 h. The last example as well as the other aforementioned are controlled by electricity. If controlled operation is not necessary, a drug delivery device can be even more simple, as illustrated in the following.

Osmosis is a very well established actuation principle for drug delivery devices [13]. The osmotic flow across a semipermeable membrane can be transformed into mechanical work. This work can be utilized to transport fluids into the body. One device [14] generates a flow rate of 1 $\mu\text{l h}^{-1}$ operating for approximately 1 year. It is rod shaped (diameter min. 1.43 cm, length min. 11.0 cm) which is supposed to be an inappropriate shape for a medical device⁸. Another one [15] uses an osmoregulatory principle to generate a constant flow rate. The dimensions of the device are 6.8 cm × 3.0 cm × 4.5 cm with potential for further miniaturization. A flow rate of 32 $\mu\text{l h}^{-1}$ was reported. Due to the osmoregulatory principle, the pump is able to transport a liquid volume more than 40 times larger than the volume of the salt chamber.

A complementary approach is the use of superabsorbent polymers (SAP). These polymers consist e.g. of partially neutralized polyacrylic acid chains crosslinked to a network [16]. After taking up some water, the SAP granulate forms a

hydrogel. Either the SAP granulate or the hydrogel can be used for the design of actuators for drug delivery applications, as explained in the following.

Hydrogels can perform mechanical work as a result of a pH change. A device based on this effect is presented in [17]. It operates with a flow rate of 2 $\mu\text{l h}^{-1}$ for 12 h.

A drug delivery device with a time delay mechanism [18] uses SAPs that were originally developed for hygiene applications. To achieve a linear volume expansion over time, the authors controlled the supply of swelling agent to the SAP. Additionally, the authors added a time delay mechanism based on a friction piston. The high counter force of the friction piston reduced the speed of the swelling process. After a certain distance, the diameter of the cylinder increased, leading also to an increased speed of swelling induced volume expansion. Due to this piston based mechanism the device shows an unfavourable rod shaped design. It can pump a fluid at a flow rate of 250 $\mu\text{l h}^{-1}$ for 2 h. The time delay functionality may help in dealing with the dawn phenomenon⁹ of diabetic patients or it might enable other chronotherapeutic [19] applications.

In this paper we introduce a flat design for a SAP actuator which is able to expand continuously for several hours. It can be manufactured easily at anticipated low costs and it enables a more convenient light weight and flat device design. We studied the influence of two device parameters (hardness of the elastic membrane separating the actuator from the drug reservoir and device diameter) and different SAP types on the actuator swelling kinetics. One design was identified that shows approximately zero order kinetics for more than 4 h. Such a characteristic is supposed to be ideal for a drug delivery device. The back-pressure sensitivity of this actuator is studied and presented. Finally, we demonstrate a skin attachable drug delivery device employing the proposed SAP actuator. This device integrates the SAP actuator, an activation mechanism and a drug pouch containing the infusion solution. The performance and operability of the suggested design is checked with experiments.

2. Actuator design

SAPs are hard dry powders. They can absorb an amount of water up to several hundred times their dry weight. As a consequence, a soft and rubbery hydrogel is formed. Unlike other absorbent materials, SAP gels will not release the water when squeezed with the fingers [16].

The most common type of SAP is a crosslinked network of partially neutralized (sodium) polyacrylic acid. The presence of the polymeric ions results in strong absorption properties because the ions are strongly solvated due to the ion–dipole interactions with water molecules [16]. The swelling kinetics is influenced by chemical properties: type of monomer, type of covalently bound ionic group, type of counterion, degree of neutralization and number of crosslinks. Additionally, physical properties like SAP particle size distribution and shape also affect the swelling properties.

⁴ Ultraflow infusion pump by Fresenius Kabi, Bad Homburg, Germany, www.fresenius-kabi.com.

⁵ ON-Q elastomeric reservoir pump by I-Flow, Lake Forest, USA, www.iflo.com.

⁶ Ambix Anapa, Fresenius Kabi, Bad Homburg, Germany, www.fresenius-kabi.com.

⁷ PatchPump by Steadymed, Tel-Aviv, Israel, www.steadymed.com.

⁸ The device was not developed for medical purposes.

⁹ Increase in blood sugar usually between 2 and 8 am.

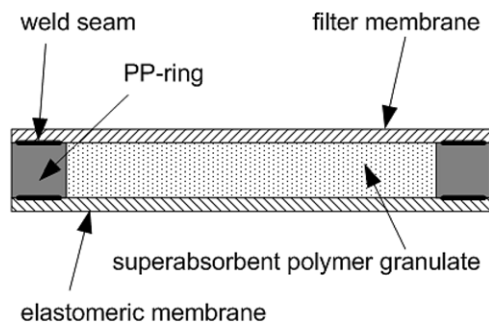


Figure 1. Illustration of the cross section of a superabsorbent polymer actuator. The cavity of the ring made of PP is filled with granulate of superabsorbent polymer. It is closed by welding a filter (polyester mesh) at the top and an elastomeric membrane at the bottom of the ring surface.

In general, the swelling rate of a SAP polymer is fast in the beginning of the absorption process. With time the swelling ratio decreases. There are polymers that absorb a large fraction of the theoretically absorbable mass very fast. Other polymers show a substantial reduction in swelling rate after absorption of a small fraction of the theoretically absorbable mass. The influence of the chemical and physical properties on the swelling kinetics of the polymer are reviewed and explained in detail e.g. in [16] or [20]. The fast reduction in swelling rate after absorption of a small fraction of the theoretically absorbable mass can be caused by so-called gel-blocking. It occurs when the outer surface of a tightly packed mass of fine particles swells too quickly [16]. It results in a reduction of the interparticle porosity. This reduces or prevents the penetration of the liquid into the interior particles. The swelling rate reduces to the diffusion rate of the liquid through the partially swollen mass.

We propose a flat and simple SAP actuator structure. Its cross section is illustrated in figure 1. It consists of a polypropylene (PP) ring. Its cavity is filled with SAP granulate. It is closed on one side with a thermoplastic elastomeric membrane and on the other side with a woven polyester mesh. This mesh is a rigid filter which is supposed to keep the SAP granulate and the hydrogel in the cavity. The mesh and the elastic membrane are bonded to the PP ring by plastics welding.

Fabrication is already quite simple. Nevertheless, mass fabrication can be even simpler. One could think of the following three steps. First: two component injection moulding of the ring and the thermoplastic membrane; second: filling with SAP granulate; and third: sealing with the filter membrane.

The functional principle of the SAP actuator is simple. The swelling agent, e.g. water, can get in contact with the SAP granulate via the filter membrane. Immediately, the SAP granulate takes up the swelling agent. The swelling process is started. It continues as long as the chemical potential of the free water is higher than the chemical potential of the absorbed water. Continuously, the volume of the cavity increases by bulging the elastomeric membrane outwards. This way the chemical energy stored in the SAP

Table 1. Internal parameters with an influence on the performance of the SAP actuator.

Geometrical factors	Material properties
Filter pore size	Type of SAP
Cavity volume (diameter, height)	Amount of SAP
Thickness of the elastomeric membrane	Stiffness of the filter membrane
	Hardness of the elastomeric membrane

is transformed into mechanical work. Anything (solid, liquid or gaseous) moveable on the other side of the elastomeric membrane can be displaced.

The capacity of the SAP actuator to take up swelling agent and its transient behaviour are influenced by external and internal parameters. External parameters are the chemical potential of the swelling agent, the external pressure on the elastomeric membrane, and the input and output flow rate. The temperature is another external parameter that is not investigated in this work. Numerous internal parameters of the SAP actuator are listed in table 1. They can be influenced by design. The main objective of this paper is to characterize the influence of important factors on the performance of the SAP volume displacement actuator. This is done with a factor screening experiment.

3. Materials and methods

PP rings with an outer diameter of 40 mm and inner diameters of 17 mm (area 2.3 cm²), 19.5 mm (area 3.0 cm²) and 24 mm (area 4.5 cm²) were manufactured by laser cutting of PP sheets (thickness 1, 1.5 or 2 mm, obtained from Schmidt & Bartl, Villingen-Schwenningen, Germany). The volume of the ring cavity is always 0.45 ml. The edges were deburred manually. Actuator fabrication started by welding the polyester mesh (mesh opening 40, 50 or 105 μm, Spectrum Laboratories, Rancho Dominguez, CA, USA) to the PP ring. A ring shaped hot welding tool (240 °C) with an appropriate inner diameter and a width of 2 mm was used. It was pressed against the mesh and the PP ring with a pneumatic cylinder (pressure 400 kPa, time 5 s, custom made at HSG-IMIT). Then, the cavity volume was filled with SAP granulate (SXFines, SXM 9410 or VPFines, Favor, Evonik Stockhausen, Krefeld, Germany; the powder density of the granulate is in the range of 0.5–0.7 g cm⁻³). The (Favor) granulate is a product based on partially neutralized and crosslinked (sodium) polyacrylic acid. The granulates of type SXFines (average particle diameter <150 μm) and SXM 9410 (average particle diameter 150–850 μm) consist of surface crosslinked particles. Particles of type VPFines (average particle diameter < 150 μm) are not surface crosslinked. The SAP actuator was closed by welding the elastomeric membrane (thickness of 0.25 mm, hardness Shore A30, A50 or A70, custom made by Tekni-Plex Europe, Erembodegem, Belgium) to it (figure 3(a)). Figure 2(b) demonstrates the volume change of a SAP actuator after swelling for several days.

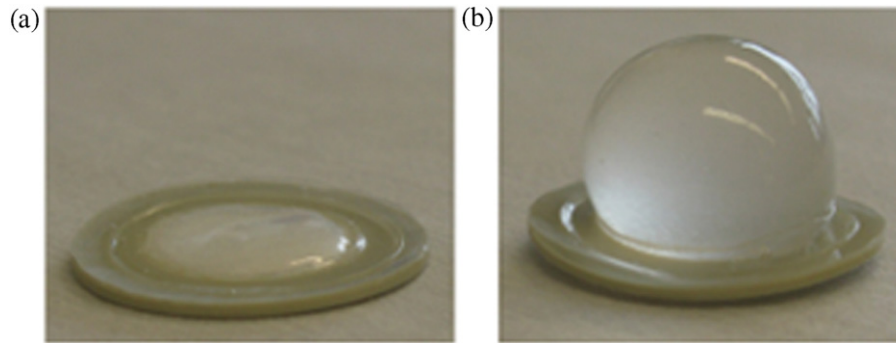


Figure 2. (a) Completely assembled SAP actuator (inner- \varnothing : 17 mm, outer- \varnothing : 30 mm) with elastomeric membrane (thickness: 0.25 mm, hardness: 50 Shore A) upside and filled with 0.1 g of SAP granulate (VPFines Favor). (b) SAP actuator swollen to a volume of approximately 3 ml after three days.

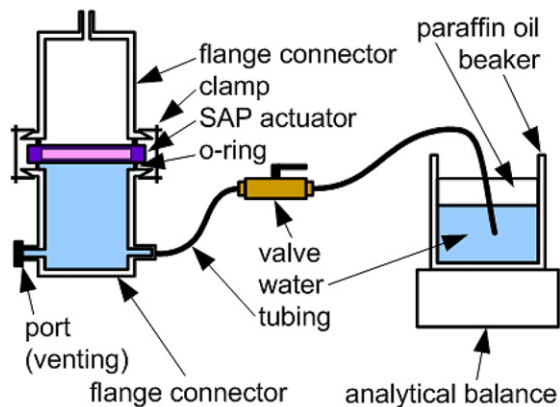


Figure 3. Experimental set-up to study the dynamics of the volume displacement of the SAP actuator at ambient pressure. The SAP actuator is mounted between two flange connectors made of glass via two o-rings and a clamp. The bottom flange connector is filled with water. Tubing connects the flange connector with a beaker which also contains water and paraffin oil (to prevent evaporation). The beaker is placed on an analytical balance.

The experimental set-up to study the dynamics of the volume displacement of the SAP actuator is shown in figure 3. The actuator is mounted on a water filled flange connector made of glass (custom made by a local glassblower). Tubing (fluorinated ethylene propylene—FEP with inner- \varnothing : 0.8 mm, length approximately: 50 cm) connects the flange connector with a water filled beaker on an analytical balance (AC 210 S, readability 0.1 mg, Sartorius, Göttingen, Germany). The balance is connected to a PC for continuous data acquisition. The water surface in the beaker is covered with paraffin oil (Sigma-Aldrich, Munich, Germany) to prevent evaporation.

Experiments were started by dosing 2 or 10 ml of deionized (DI) water into the cavity of the top flange connector. It was covered (not air tight) with a lid to prevent evaporation but permit venting.

After dosing DI water to the actuator it passed immediately the filter membrane and reached the SAP granulate. Instantaneously, the transient swelling process of the particular actuator under tests starts. As a consequence the elastomeric membrane bulged and pushed the water in the flange connector through the tubing into the beaker on

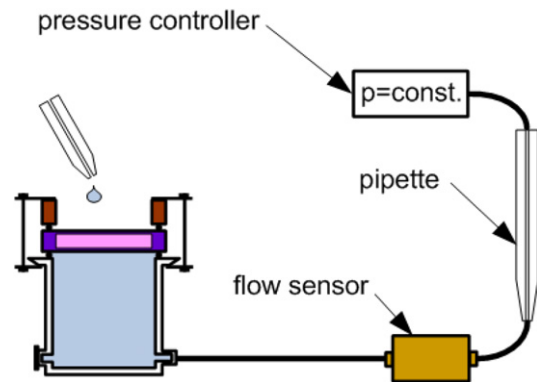


Figure 4. Experimental set-up to study the dynamics of the volume displacement of SAP actuators at defined back-pressures. Tubing connects the flange connector with a flow sensor, a pipette and a pressure controller.

the analytical balance. The transient increase in mass was recorded.

The set-up with analytical balance is very accurate with regard to absolute values. However, it cannot be used to study the dynamics of the volume displacement for various back-pressures. Therefore, the set-up was modified according to figure 4. The desired back-pressure is generated with a pressure controller (DPI530, range 200 kPa, GE Sensing, Fairfield, CT, USA). The displacement of water is acquired with a mass flow sensor (LiquiFlow, range 6 g h^{-1} , Bronkhorst, Ruurlo, The Netherlands). The suggested set-up is prone to offset errors of the flow sensor. Hence, a pipette (2 ml) was used to get the absolute displacement in order to check the integrated data of the flow sensor. The working fluid of the pressure controller is air. Thus, the set-up was configured in a way that the phase boundary water/air was located at the bottom of the pipette before an experiment was started.

4. Results and discussion

4.1. Initial experiments

A first series of initial experiments was done to get an impression of the transient volume displacement of SAP

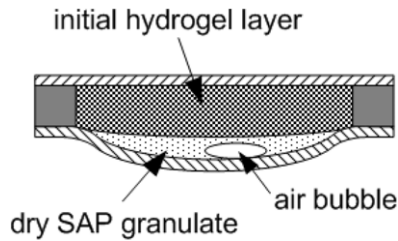


Figure 5. State of a SAP actuator with VPFines after the experiment. A layer of dry SAP pellets and an entrapped air bubble could be seen through the opaque elastomeric membrane.

actuators filled with different types of SAP (SXFines, SXM 9410 and VPFines). Except for the type of SAP, all other design parameters and ambient conditions were kept constant (inner- \varnothing : 17 mm, thickness of PP ring: 1 mm, mesh opening: 105 μm , thickness of elastomeric membrane: 0.25 mm, hardness of elastomeric membrane: Shore A50, amount of SAP: 0.1 g, room temperature, ambient pressure).

Three actuators per SAP type were investigated after delivering 2 ml of DI water. The volume displacement of each of them was recorded for 4 h. After each experiment the actuator was removed from the set-up and inspected. The elastic membrane bulged outward as expected. The filter membrane retained the hydrogel in the cavity. However, its surface felt greasy. This indicates that hydrogel reaches partly across the filter pores without losing its connection to the gel inside the cavity. Apart from that, the filter membrane also bulged out slightly. Hence, the efficiency in volume displacement of the actuator is not ideal. A layer of dry SAP pellets and an entrapped air bubble could be seen through the opaque elastomeric membrane of actuators filled with VPFines (figure 5). The SAP granulate of the other polymers formed a homogeneous gel and a distinct air bubble could not be detected. In this case either the air or some of it could escape the actuator or it is evenly distributed in the gel.

The result of the initial series of experiments obtained with the experimental set-up (figure 3) is presented in figure 6. The displaced volume within 4 h ranges from 0.77 ml \pm 0.06 ml for VPFines to 0.92 ml \pm 0.08 ml for SXFines. The main difference between the three polymers is their behaviour in the early phase. The three configurations show large differences in terms of how fast they react on the addition of swelling agent. Consequently they show large differences in the displaced volume during that initial phase (5 min). The smallest initial displacement was observed with VPFines (0.12 ml \pm 0.03 ml) and the highest initial displacement was observed with SXFines (0.52 ml \pm 0.08 ml).

The small initial displacement with VPFines can be explained by the fast formation of a dense gel layer. Water needs to diffuse through this gel layer to reach the dry SAP pellets. Apparently this is gel-blocking.

To extract quantitative information regarding the duration of the initial volume displacement phase the data were fitted to the following equation:

$$f(t) = \alpha(1 - e^{-\frac{t}{\tau_1}}) + \beta(1 - e^{-\frac{1}{\tau_2}}). \quad (1)$$

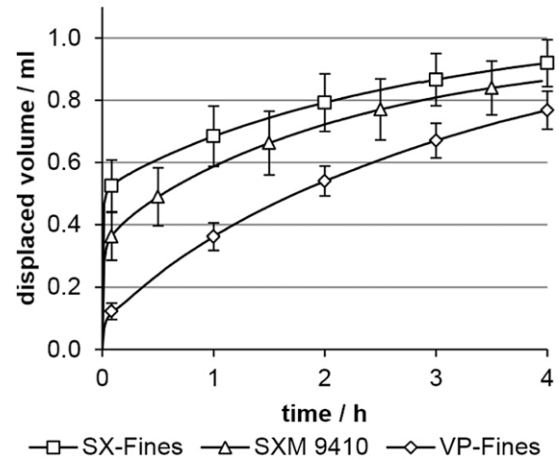


Figure 6. Transient behaviour of the volume displacement of SAP actuators filled with different superabsorbent polymer pellets. The mean of three SAP actuators and the standard deviation (at selected points) is plotted.

This empiric equation describes the displaced volume versus time as a superposition of two dynamic effects modelled with asymptotic exponentials. $f(t)$ is the displaced volume at time t , α and β are the asymptotic values and τ_1 as well as τ_2 equals the time until 63% of the asymptotic value is reached. The experimental data fits very well to equation (1) with coefficients of determination of 0.99 and higher. The longest duration τ_1 of the graphs of figure 6 is 1.2 min (VPFines). Thus, within 3.6 min (three times τ_1) the volume displacement in the initial phase reached at least 95% of its final value. τ_2 ranges from 126 to 162 min.

Based on this data, two types of SAP were allocated to two levels for the factor screening experiment presented in section 4.2. VPFines was allocated to level 1 because the volume displacement during the initial phase is very low. SXFines was allocated to level 1 because the volume displacement during the initial phase is large.

4.2. Factor screening

4.2.1. Design of the experiment. A factor screening experiment was set up to identify and study the influence of relevant design parameters on the transient volume displacement of the actuator. Two response variables of the screening experiment were extracted from the displaced volume over time. The first variable is the displaced volume after 5 min (V5); the second one is the gain at 4 h (G235) which represents the displaced volume between 5 min and 4 h. The selected factors, their levels and ranges are given in table 2.

Factor A is the filter area of the SAP volume displacement actuator. The filter area, its diameter and the volume of the actuator cavity are dependent dimensions. Therefore, diameters (17, 19.5 and 24 mm) were selected that result in the same cavity volume (0.45 ml) when PP sheets with a thickness of 1.0, 1.5 and 2.0 mm were used. The medium level of factor A (filter area) is -0.32 . It is not zero because the area of

Table 3. Experimental design and results of the 2³ factorial design with double replication and additional ‘centre’ points. (Data presented without randomization.)

Set	Factor levels			Response variables of displaced volume ml ⁻¹			
	A	B	C	After 5 min (V5)		5–235 min (G235)	
				1	2	1	2
1	−1	−1	−1	0.155	0.189	1.005	0.978
2	−1	−1	1	0.117	0.072	0.850	0.843
3	−1	1	−1	0.955	0.856	0.818	0.870
4	−1	1	1	0.470	0.460	0.803	0.800
5	−0.32	−1	0	0.277	0.322	1.141	1.134
6	1	−1	−1	0.363	0.317	1.837	1.577
7	1	−1	1	0.208	0.200	1.447	1.479
8	1	1	−1	2.392	2.267	1.452	1.327
9	1	1	1	1.103	1.104	1.136	1.160
10	−0.32	1	0	0.813	0.878	1.067	0.965

Table 2. Levels of the design factors.

Factors	Levels		
	−1	−0.32/0	1
A Filter area (inner diameter)	2.3 cm ² (17 mm)	3.0 cm ² (19.5 mm)	4.5 cm ² (24 mm)
B Type of SAP	VPFines		SXFines
C Hardness of membrane	Shore A30	Shore A50	Shore A70

the medium actuator (3.0 cm²) is smaller than the mean area (3.4 cm²) of the small and the large actuator.

The actuator cavity was filled with a different mass (0.23 g VPFinnes and 0.31 g SXFinnes) of SAP due to the different powder densities. This way the cavities were completely filled with an equal volume of SAP granulate. The difference in granulate mass is not considered relevant because the SAP pellets are supposed to absorb just a tiny fraction of the theoretically absorbable mass.

The level of factor B describes the SAP material. It is set according to the results of the preliminary experiments. These results were not obtained independently of the other parameters. Therefore, just the two extremes (VPFinnes and SXFinnes) were assigned to factor levels −1 and 1. No SAP granulate was assigned to factor level 0.

The hardness of the membrane is coded with factor C. The levels were set according to the available materials. Membranes with different hardness but the same thickness (0.25 mm) were obtained.

The experiments were performed at ambient conditions in the laboratory. Thus, changes in temperature and pressure are present but small. Variations in the assembly process (e.g. variations in the position of the weld seam) might also affect the response variables. Nevertheless, all these factors were neglected.

With three factors at 2 levels (−1 and 1) a full factorial design results in 8 experiments. An additional true centre point cannot be realized because factor B is a categorical factor with just two levels. Instead, experiments with factor level combinations −0.32/−1/0 and −0.32/1/0 were added to the design (table 3).

To determine the minimum number of experiments, it is necessary to define a difference in the effect to be detected. This difference is set to 0.2 ml of volume displacement. With this level it is possible to distinguish actuators with substantially different V5 values and substantially different G235 values. The standard deviation is set to 0.07 ml according to the average of the preliminary experiments. The significance level (probability to detect a difference when there is no difference) is set to 5%. The power (probability of detecting a difference when there is a difference) is set to 80%. The maximum number of factor levels is 3. With these specifications, the minimum number of replications was determined to 4 (the no.reps function of the dae package of R was used). With double replication of the experimental design every factor level is replicated at least four times while most factor levels are replicated eight times. Overall, 20 experiments were performed.

The actuators were manufactured in blocks (depending on the filter area). Within each block fabrication was done in a randomized order. The complete experimental design is presented in table 3. The experiments were performed as described already. The data of the response variables were obtained from the transient signals and are also presented in table 3. Additionally, to get the true amount of absorbed water the actuator cavities were opened after each experiment. The gel was removed and weighed. By subtracting the dry polymer mass, one gets the desired mass of the absorbed amount of water.

4.2.2. Experimental result and data analysis. First, the absorbed amount of water was compared to the displaced volume obtained by conversion of the acquired mass data of the balance. On average the displaced volume is 74% ± 4% of the total absorbed volume. Hence, not all the absorbed volume contributes to the desired displacement. This is partly caused by superseding the air between the particles of the granulate in the actuator cavity with water, compression of the remaining air and the limited stiffness of the rigid filter membrane. Thus, one way to increase the efficiency is to use a stiffer filter membrane. Another way to increase the efficiency

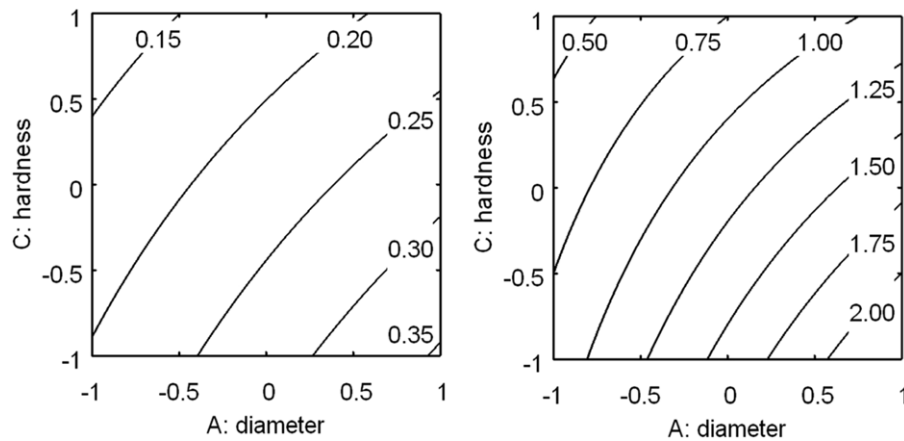


Figure 7. Response variable V5 (displaced volume after 5 min) as a function of diameter (factor A) and hardness of the elastomeric membrane (factor C) as a contour plot. Left: VPFines (factor B at level -1). Right: SXFines (factor B at level 1).

Table 4. ANOVA for the response displaced volume after 5 min.

	Sum of squares	Degrees of freedom	Mean square	F_0	P -value
Model	8.157	7	1.165	161.34	<0.0001
A	1.421	1	1.421	196.70	<0.0001
B	4.403	1	4.403	609.72	<0.0001
C	0.884	1	0.884	122.35	<0.0001
AB	0.894	1	0.894	123.77	<0.0001
AC	0.178	1	0.178	24.66	<0.0001
BC	0.528	1	0.528	73.08	<0.0001
ABC	0.132	1	0.132	18.30	0.0011
Residuals	0.087	12	0.007		
Lack of fit	0.068	2	0.034	18.34	0.0005
Pure error	0.019	10	0.002		
Cor total	8.243	19			

is to replace the air in the cavity by a suitable material or to decrease the actuator cavity volume to a minimum that is needed for a designated volume displacement.

Next, the data were analysed based on a full model considering all three single factors (A, B and C), all three two factor interactions (AB, AC and BC) and the three factor interaction (ABC). The ANOVA table for the response V5 is given in table 4. The model is significant with very low pure error. However, there is significant lack of fit. Thus, there is nonlinear curvature in the data that cannot be represented by the model. Therefore, the model is accurate in the corners of the design space and in a region close to the corners. The residual plots of the model can be found in supplement 1 and 2 (available at stacks.iop.org/SMS/21/105002/mmedia). There is no indication that the assumptions on normality and constant variance are violated. Outliers are not present.

The response G235 was analysed based on a full model. The model was reduced by removing insignificant terms. A transformation of the response with the ln function was indicated by the box cox¹⁰ method due to non-constant variance. The ANOVA table of the transformed response is

Table 5. ANOVA for the transformed response gain at 4 h.

	Sum of squares	Degrees of freedom	Mean square	F_0	P -value
Model	1.149	4	0.289	94.70	<0.0001
A	0.938	1	0.938	309.22	<0.0001
B	0.127	1	0.127	41.74	<0.0001
C	0.076	1	0.076	24.98	0.0002
AB	0.015	1	0.015	4.83	0.0442
Residuals	0.046	15	0.003		
Lack of fit	0.022	5	0.004	1.87	0.1874
Pure error	0.024	10	0.002		
Cor total	1.195	19			

presented in table 5. The model is significant with very low pure error and lack of fit is insignificant. The residuals of the transformed response G235 are plotted in supplement 3 and 4 (available at stacks.iop.org/SMS/21/105002/mmedia). The transformation solved the problem of non-constant variance (with supplement 4 available at stacks.iop.org/SMS/21/105002/mmedia, right as a potential exception). The assumption of normality is acknowledged and outliers could not be identified.

The full model of the data V5 is shown in figure 7. The left contour plot shows the model with factor B (type of SAP) at level -1 ; the right contour plot shows the model with factor B (type of SAP) at level 1. The model standard deviation is ± 0.09 g. With factor B (type of SAP) at level -1 (VPFines) there is much less influence of factor A (diameter) and factor C (hardness of membrane) on V5 compared to level 1 (SXFines).

The back transformed reduced model of the data G235 is shown in figure 8. The left contour plot shows the model with factor B (type of SAP) at level -1 (VPFines); the right contour plot shows the model with factor B (type of SAP) at level 1 (SXFines). The model standard deviation was calculated explicitly at data points of the transformed model and back transformed to the original scale. It ranges from 0.05 to 0.10 ml with factor B at level -1 and from 0.04 to 0.08 ml with factor B at level 1.

¹⁰ The boxcox function of the MASS package of R was used.

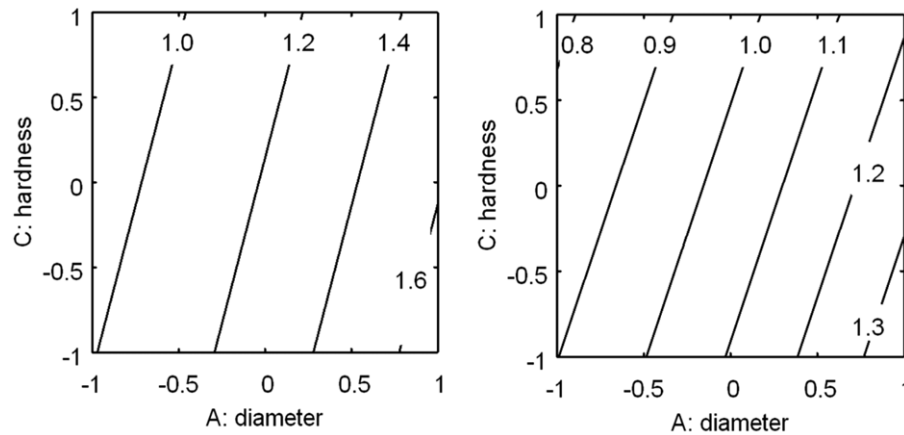


Figure 8. Response variable G235 (displaced volume between 5 min and 4 h) as a function of diameter (factor A) and hardness (factor C) as a contour plot. Left: VPFines (factor B at level -1). Right: SXFines (factor B at level 1).

With factor B (type of SAP) at level -1 (VPFines) the V5 value (figure 7) is significantly smaller than with factor B (type of SAP) at level 1 (SXFines) regardless of the level of factors A (filter area) and C (hardness of membrane). This is explained by the fast formation of a dense gel layer with VPFines (level -1) compared to SXFines (level 1) as already explained (see section 4.1). Thus, to get a volume displacement actuator with a small value of V5, it is beneficial to set factor B (type of SAP) to level -1 (VPFines).

The highest values of G235 can be achieved with factor B (type of SAP) set to level -1 (VPFines). This becomes clear by comparing the contour plots of figure 8. Thus, both goals, minimized V5 and maximized G235, can be accomplished with factor B (type of SAP) at level -1 (VPFines).

The levels of factors A (filter area) and C (hardness of membrane) are contradictory concerning the minimization of V5 and maximization of G235. This becomes clear from the nature of these factors. If the filter area is larger, the flow of water into the actuator is higher. Consequently, V5 as well as G235 is increasing. If the hardness of the elastomeric membrane increases, the pressure inside the actuator cavity is higher at identical cavity volumes. Thus, if the swelling process is influenced by the pressure in the cavity, V5 as well as G235 is reduced if a membrane with a higher hardness is used.

4.2.3. Test of the model. To demonstrate the predictive capability of the model, 4 experiments with two parameter sets not included in the designed experiment were performed. The first parameter set (A: -0.32 , B: -1 and C: 1) should result in a quite low V5 with a predicted range of $0.16 \text{ ml} \pm 0.09 \text{ ml}$ and a reasonable G235 with a predicted range of $1.03 \text{ ml} \pm 0.06 \text{ ml}$. The V5 of the two performed experiments is 0.15 ml and 0.14 ml . Both are within the predicted range. The G235 was experimentally determined to be 1.19 and 1.07 ml . Thus, the first result is larger ($+0.1 \text{ ml}$) than the predicted range. However, the deviation from the model is smaller than the difference in effect to be detected (0.2 ml) defined in the design of the experiment

(section 4.2.1). The second parameter set (A: 1, B: -1 and C: 0) should result in a moderate V5 with a predicted range of $0.29 \text{ ml} \pm 0.09 \text{ ml}$ and a high G235 with a predicted range of $1.59 \text{ ml} \pm 0.09 \text{ ml}$. The V5 of the two experiments resulted in 0.33 and 0.29 ml . Both are inside the predicted interval. The G235 is 1.56 ml and 1.66 ml . Both values are in the predicted interval. The performed tests demonstrated the capabilities of the models that live up to the defined expectations.

4.3. Volume displacement with back-pressure

The influence of back-pressure on the volume displacement process of SAP actuators was studied at 5 pressure levels from 50 to 200 kPa. The following actuator design was selected. The inner diameter was set to 17 mm (level A at -1). The polymer VPFines was used (factor B at level -1). An elastomeric membrane with shore hardness of A50 was selected (factor C at level 0). Apart from the previous actuator designs the mass of SAP polymer was set to 0.1 g and the mesh width of the filter membrane was set to $50 \mu\text{m}$. According to the model the selected actuator design is supposed to show a small V5 of $0.17 \text{ ml} \pm 0.09 \text{ ml}$ and a moderate G235 value of $0.93 \text{ ml} \pm 0.05 \text{ ml}$ at 0 kPa back-pressure.

Twenty actuators were studied at four pressure levels ranging from 50 to 200 kPa (figure 9). A linear fit to the data results in coefficients of determination from 0.94 to 1.00 (fits with y-axis-intercept = 0 result in coefficients of determination from 0.75 to 1.00). Hence, the displacement of volume shows approximately zero order kinetics within the first 4 h. The approximation is supposed to be adequate for drug delivery devices. The same data are presented as a function of back-pressure after 4 h in figure 10. The G235 value drops from a level of $0.81 \text{ ml} \pm 0.03 \text{ ml}$ at 50 kPa to $0.28 \text{ ml} \pm 0.06 \text{ ml}$ at 200 kPa. The data fit very well to a straight line with a coefficient of determination of 0.99. The extrapolated volume displacement for a back-pressure of 0 Pa is 1.00 ml . It is just slightly higher than the predicted value of $0.93 \text{ ml} \pm 0.05 \text{ ml}$. This is remarkable because the mass of SAP is lower compared to the actuators used in the factor

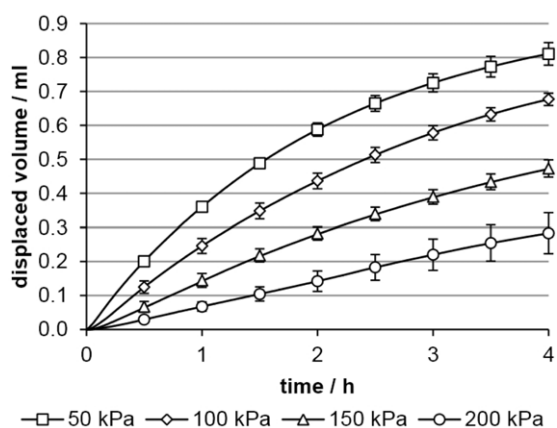


Figure 9. Transient behaviour of the volume displacement of SAP actuators at different back-pressures. The mean of five SAP actuators and the standard deviation (at selected points) is plotted.

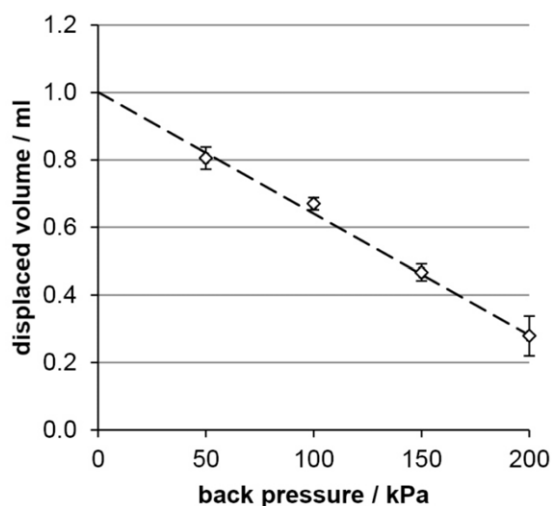


Figure 10. Displaced volume between 5 and 235 min (G235) as a function of back-pressure.

screening experiment. It supports the argument stated at the beginning of this paper: changes in the mass of the SAP are less relevant.

5. Skin attachable drug delivery device

An implementation of a drug delivery device with an integrated SAP actuator is presented in figure 11. The SAP actuator is placed between the activation mechanism and the drug pouch within a case. The activation mechanism consists of the expanding agent pouch, the check valve, the delay pouch and the delay pellet. The drug pouch is connected to an intradermal infusion set with a cannula¹¹. If the SAP actuator expands it compresses the drug pouch and its content is delivered through the cannula to the skin of the patient.

¹¹ The pressure in the filled drug pouch (1.7 ml, width and length of storage compartment: 25 mm × 35 mm) is 1.2 kPa. In combination with a cannula (length 30 mm, inner diameter 0.13 mm) there is a liquid flow after removal of the rubber cap of 16 $\mu\text{l min}^{-1}$. This is not considered relevant.

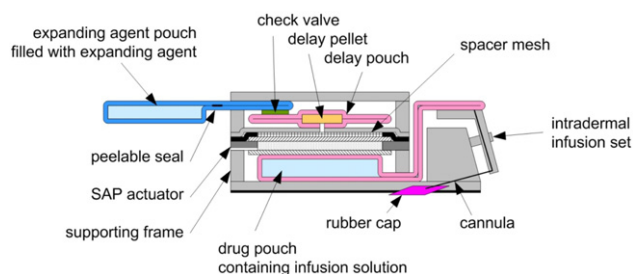


Figure 11. Detailed view of a skin attachable drug delivery device and its components. The components are explained in the text.

The activation mechanism contains a delay pellet made of a sucrose melt. By proper design of the delay pellet and adequate selection of sucrose concentration in the expanding agent the delay time can be adjusted between minutes to hours. A short delay time can be helpful during the activation of the device whereas a long delay time can be used for chronotherapeutic applications. Additionally, the delay pellet permits evacuation of the delay pouch. This is important to prevent air bubbles that otherwise can occur after transferring the expanding agent from its pouch to the delay pouch.

Figure 11 shows the device during storage (step I). The activation procedure starts by removing the rubber cap, fixation of the device on the skin surface and placing of the cannula in the skin (figure 12, step II). Next, the expanding agent needs to be transferred to the delay pouch. This is done by squeezing the expanding agent pouch manually. Accordingly, the peelable seal opens and the liquid is transferred through the check valve (step III). Optionally, the expanding agent pouch can be removed, now. The check valve keeps the expanding agent in the delay pouch. Next, the delay pellet dissolves within a certain time. After this process the passage between the delay pouch and the SAP actuator is free (step IV). Now, the expanding agent can enter the SAP actuator where it is absorbed by the SAP granulate. As a consequence the volume of the SAP actuator increases and deflects the elastomeric membrane. Thereby, it squeezes the drug pouch. Hence, the drug solution is transported via the cannula of the intradermal infusion set into the patient's skin (step V).

Several delivery devices were assembled to prove the device concept (functional model presented in figure 13, functional model with cover and intradermal infusion set presented in supplement 5 available at stacks.iop.org/SMS/21/105002/mmedia). The drug pouch (a detailed sketch can be found in supplement 6 available at stacks.iop.org/SMS/21/105002/mmedia) was manufactured from polyethylene (PE) film with a thickness of 0.1 mm. The width and length of the (flat and empty) storage compartment is 25 mm × 30 mm. The SAP actuator (diameter: 17 mm, thickness 1 mm) is placed on a 2 mm thick supporting frame above the drug pouch. It was filled with 0.16 g SAP granulate (SXM 9410), and sealed by an elastomeric membrane (Shore A 30) on one side and a polyester mesh (40 μm mesh opening) on the other side. A spacer mesh (PP, 0.3 mm mesh opening) was placed on top of the SAP actuator. It enables the expanding agent

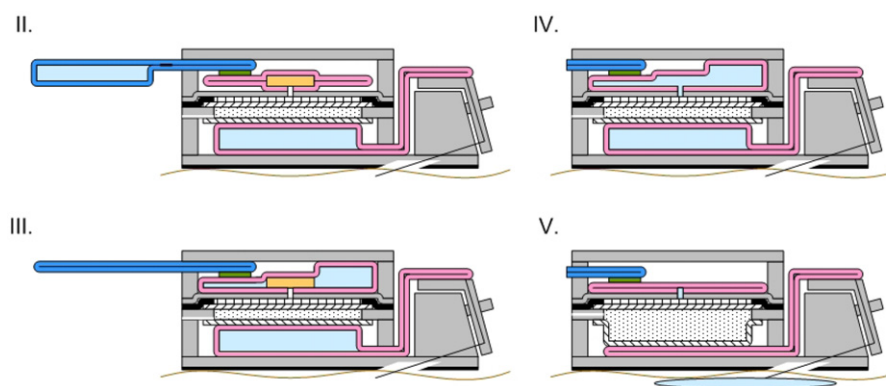


Figure 12. Subsequent steps of device usage. (Step I: device during storage, and the labelled components are presented in figure 11.) Step II: the cannula of the intradermal infusion set is inserted into the skin. Step III: the content of the expanding agent pouch is transferred to the delay pouch. Step IV: the delay pellet is completely dissolved. Step V: the expanding agent is absorbed by the SAP actuator and the content of the drug pouch is infused into the skin.

to enter the hydrogel actuator via the full actuator surface. The delay pellet (diameter: 12 mm, thickness: 1.6 mm, supplement 7 available at stacks.iop.org/SMS/21/105002/mmedia) is mounted in the delay pouch (PE film, thickness: 0.1 mm, width and length: 25 mm × 30 mm) with double side adhesive. This way the opening facing to the SAP actuator was covered. The delay pouch was evacuated and the last weld seam was generated in a vacuum packaging machine. Of course, the check valve and the expanding agent pouch were already mounted to the delay pouch. Otherwise, it would not be possible to generate a vacuum in the delay pouch. The check valve (supplement 8 available at stacks.iop.org/SMS/21/105002/mmedia) is assembled from an elastomeric membrane and PP film (thickness 0.3 mm). A cut ($\approx 2\text{--}3$ mm) in the elastomeric membrane is located off centre to a hole (diameter 1.5 mm) in the PP film. Thus, fluid flow is blocked in one direction if the elastomeric film is pressed to the PP film. In the other direction fluid flow occurs after a small deformation of the elastomeric film results in a conduit. The expanding agent pouch (width: 25 mm, length: variable, supplement 9 available at stacks.iop.org/SMS/21/105002/mmedia) is manufactured from translucent peel film (1275.PPT.000, Orbita Film, Weißandt-Gölzau, Germany). The peelable seal was generated with a wedge shaped welding tool (width 1.5 mm, angle 90°) at 160°C (200 kPa, 5 s). The permanent seals were generated at a much higher temperature. The last weld seam was generated after filling with 2 ml of expanding agent (DI water). If pressure is applied to the expanding agent pouch the maximum stress is at the corner of the peelable seal. With this geometrical feature the pressure necessary to open the expanding agent pouch is reduced to an acceptable level. For reliable activation of the delivery device it was necessary to introduce venting cannulas that reach into the SAP actuator. Without these cannulas the confined air in the actuator can prevent the expanding agent from entering the SAP actuator.

To characterize the assembled device depicted in figure 13 the drug pouch was connected to an adapter instead of an infusion set. A tube was connected to the adapter. The free end of the tube was placed in a beaker on scales.

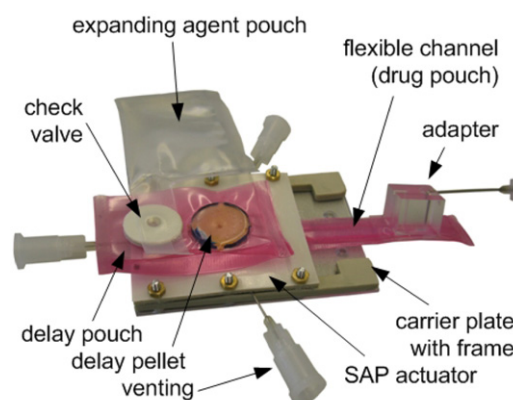


Figure 13. Assembled functional model of the delivery device with integrated SAP actuator (cover removed). The dimensions of the carrier plate are 50 mm × 30 mm. With cover the thickness is 10 mm.

The water level of the beaker is ≈ 12 cm above the device. This corresponds to a pressure of 1.2 kPa. The scales were connected to a PC for continuous data acquisition. After activation of the device the time delay and the delivered volume were recorded by the scales. The experiments resulted in a delay time of $32 \text{ min} \pm 7 \text{ min}$ ($n = 3$) and a delivered volume of $0.51 \text{ ml} \pm 0.08 \text{ ml}$ ($n = 3$) in 2 h and $0.54 \text{ ml} \pm 0.07 \text{ ml}$ ($n = 3$) in 4 h. Thus, most of the fluid was delivered within 2 h.

The delivered volume of $0.54 \text{ ml} \pm 0.07 \text{ ml}$ is a fraction of the 1.7 ml of liquid volume in the drug pouch. However, it is larger than the volume of 0.45 ml (diameter: 17 mm, height: 2 mm) underneath the elastomeric membrane of the SAP actuator. This is due to the rigidity of the PE film used for the drug pouch. With this experiment it was demonstrated that the proposed SAP actuator can be used in a small and flat drug delivery device. Further research on the pouch geometry and its interaction with the SAP actuator is necessary to improve delivery efficacy. It is also necessary to study the influence of the sucrose solution on the actuator performance.

6. Conclusions

In this paper we characterized flat SAP volume displacement actuators. In initial experiments some of the actuators showed a substantial fast displacement of volume in the first 5 min followed by a slow but continuous increase of displaced mass for more than 4 h. With a factor screening experiment the influence of the type of polymer, the hardness of the elastomeric membrane mediating the volume displacement and the filter area on the actuator performance were studied. The results enable the identification of a parameter set for an SAP actuator having a low displaced volume V_5 after the initial phase of 5 min and a large displaced volume G_{235} from 5 min to 4 h. This enables adaptation of the parameters to specific needs of a desired application. Manufacturing can be as simple as suggested with anticipated low fabrication costs. An actuator design that shows almost zero order kinetics was studied further and its back-pressure dependent volume displacement was characterized. It might be neglected in applications with small variations in back-pressure (e.g. <25 kPa).

With their ability to displace relevant volumes of liquid even against an elevated pressure level (e.g. 100 kPa), SAP volume displacement actuators can enable the realization of thin skin attached drug delivery devices. A volume of approximately 1 ml can be delivered within 4 h or faster if necessary. This was demonstrated by integration of the SAP actuator, an activation mechanism and a drug reservoir. Experimental results confirmed the utility of the device. However, further research is required to better understand the device performance. Once these tasks are finished we expect very cost effective and environment-friendly (no electronics, no battery) solutions for skin attachable drug delivery devices.

Acknowledgments

We gratefully acknowledge financial support from the Landesstiftung Baden-Württemberg (contract number 4-4332.62-HSG/34). We are also highly grateful to Evonik Stockhausen GmbH for providing us with SAP and to Orbita Film GmbH for providing us with peelable film. Moreover, we are grateful to Carolin Schmidt and Vesela Ilieva.

References

- [1] Santus G and Baker R W 1995 Osmotic drug delivery: a review of the patent literature *J. Control. Release* **35** 1–21
- [2] Prausnitz M R and Langer R 2008 Transdermal drug delivery *Nature Biotechnol.* **26** 1261–8
- [3] Griss P and Stemme G 2003 Side-opened out-of-plane microneedles for microfluidic transdermal liquid transfer *J. Microelectromech. Syst.* **12** 296–301
- [4] Vosseler M, Jugl M and Zengerle R 2010 A smart interface for reliable intradermal injection and infusion of high and low viscosity solutions *Pharm. Res.* **28** 647–61
- [5] Häfeli U O, Mokhtari A, Liepmann D and Stoeber B 2009 *In vivo* evaluation of a microneedle-based miniature syringe for intradermal drug delivery *Biomed. Microdev.* **11** 943–50
- [6] Capes D, Martin K and Underwood R 1997 Performance of a restrictive flow device and an electronic syringe driver for continuous subcutaneous infusion *J. Pain Symptom Manage.* **14** 210–7
- [7] Ma B, Liu S, Gan Z, Liu G, Cai X, Zhang H and Yang Z 2006 A PZT insulin pump integrated with a silicon microneedle array for transdermal drug delivery *Microfluid. Nanofluid.* **2** 417–23
- [8] Nisar A, Afzulpurkar N, Mahaisavariya B and Tuantranont A 2007 MEMS-based micropumps in drug delivery and biomedical applications *Sensors Actuators B* **130** 917–42
- [9] Iverson B D and Garimella S V 2008 Recent advances in microscale pumping technologies: a review and evaluation *Microfluid. Nanofluid.* **5** 145–74
- [10] Nordquist L, Roxhed N, Griss P and Stemme G 2007 Novel microneedle patches for active insulin delivery are efficient in maintaining glycaemic control: an initial comparison with subcutaneous administration *Pharm. Res.* **24** 1381–8
- [11] Meehan E, Gross Y, Davidson D, Martin M and Tsals I 1996 A microinfusor device for the delivery of therapeutic levels of peptides and macromolecules *J. Control. Release* **46** 107–16
- [12] Lynch P M, Butler J, Huerta D, Tsals I, Davidson D and Hamm S 2000 A pharmacokinetic and tolerability evaluation of two continuous subcutaneous infusion systems compared to an oral controlled-release morphine *J. Pain Symptom Manage.* **19** 348–56
- [13] Herrlich S, Spieth S, Messner S and Zengerle R 2012 Osmotic micropumps for drug delivery *Adv. Drug Deliv. Rev.* doi:10.1016/j.addr.2012.02.003
- [14] Deem T, Ligrani P M, Tower D and Connelly J 2007 Osmotic dispense pump for operation at different temperatures and pressures *Sensors Actuators A* **136** 742–8
- [15] Ehwald M, Adleff H, Geggier P and Ehwald R 2006 A long-term stable and adjustable osmotic pump for small volume flow based on principles of phloem loading *Biotechnol. Bioeng.* **94** 37–42
- [16] Allen D S, Buchholz F L, Cutié S S, Graham A T, Henton D E, Reim R E, Smith P B, Staples T L and Wilson L R 1998 *Modern Superabsorbent Polymer Technology* ed F L Buchholz and A T Graham (Hoboken, NJ: Wiley)
- [17] Eddington D T and Beebe D J 2005 Development of a disposable infusion system for the delivery of protein therapeutics *Biomed. Microdev.* **7** 223–30
- [18] Richter A, Klenke C and Arndt K F 2004 Adjustable low dynamic pumps based on hydrogels *Macromol. Symp.* **04** 377–84
- [19] Lemmer B 2007 Chronobiology, drug delivery, and chronotherapeutics *Adv. Drug Deliv. Rev.* **59** 825–7
- [20] Omidian H, Hashemi S A, Sammes P G and Meldrum I 1998 A model for the swelling of superabsorbent polymers *Polymer* **39** 6697–704